

CONDITIONAL MOMENT CLOSURE MODELLING FOR SPARK IGNITION IN A TURBULENT N-HEPTANE SPRAY

E.S. Richardson and E. Mastorakos*

*e-mail: em257@cam.ac.uk

Cambridge University Engineering Department,
Trumpington Street, Cambridge CB2 1PZ, UK

Abstract

Ignition and flame stabilisation have been simulated in a turbulent, bluff body stabilised spray flame. A complete first order Conditional Moment Closure (CMC) model for spray combustion is presented, as well as CMC modelling for spark ignition. The new elements of the two phase model formalism and the spark ignition models are illustrated using a one dimensional spray ignition example. It is shown that the new spray terms are not significant in the flows considered, however the modelling of the mixture fraction variance equation is critical. Finally, ignition of the experimental spray burner is simulated and compared with the available data, showing reasonable qualitative agreement but over-predicting the speed of flame stabilisation.

Introduction

Deeper understanding of forced ignition and flame propagation is needed by researchers developing modelling for the design of industrial burners. The ability to model ignition of spray fuelled flow is of particular interest to manufacturers of aviation gas turbines who must satisfy certification bodies that their designs may be re-ignited at high altitude.

The numerical simulations in this paper, used to develop the Conditional Moment Closure (CMC) combustion model for ignition problems, were based on the experimental study of spark ignition and flame propagation in a swirling, bluff body stabilised spray combustor by Marchione et al. [1,2]. The configuration investigated is depicted in Fig. 1, and full details may be found in ref. [1]. The main observation of interest to this study is the global propagation process as shown in Fig. 2. The spark was located at radius, $r = 0\text{mm}$ and an axial distance from the bluff body of $z = 23\text{mm}$. The experiment used a 3mm spark gap, 200mJ electrical energy, and $400\mu\text{s}$ duration.

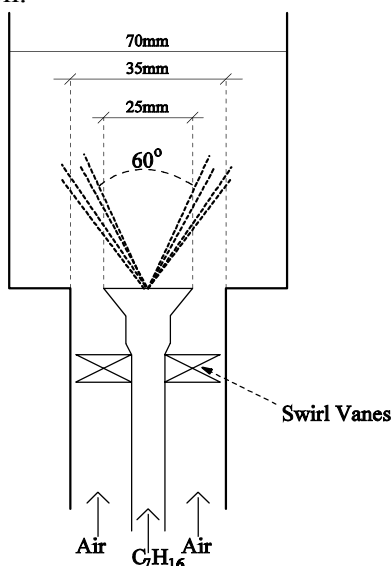


Figure 1. Schematic of burner configuration.

The CMC model is an advanced turbulent reacting flow model [3]. It has previously been applied to flame propagation problems such as igniting [4] and steady state lifted turbulent jet flames [5] and to two phase combustion in Diesel like sprays [6,7] and other applications [8,9,10]. These authors have used differing sets of CMC equations and differing approximations in their solution. Furthermore, modelling of the spray ignition experiment requires development of a spark ignition model for the CMC.

This paper starts with a presentation of a complete first order CMC two phase combustion model, including forced ignition models. The new elements of the two phase model formalism and the spark ignition models are then illustrated using a one dimensional spray ignition example. Finally, ignition of the experimental spray burner is simulated and compared with the available data.

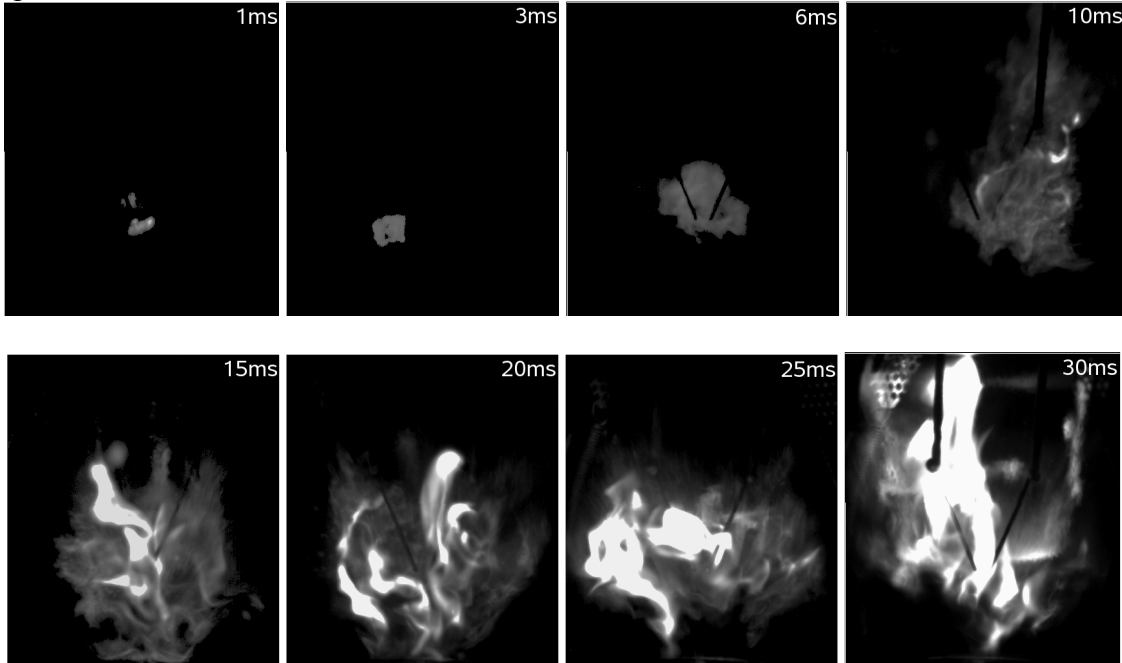


Figure 2. 2200Hz fast camera (line of sight) images of the flame evolution at the times indicated for a successful spark located at $r = 0, z = 23\text{mm}$. Spray injection is at the bottom of each image, dimensions 70mm diameter, 80mm height. Experiment by Marchione et al. [1].

Formulation

Two Phase Conditional Moment Closure Equations

The first order CMC equations for two phase flow have been employed as derived by Rogerson [8], with the conditional temperature equation provided by Richardson [10]. Conditional expectations are denoted $Q_\alpha \equiv \langle Y_\alpha | \eta = \xi \rangle$ where Y_α is the variable being averaged on the condition that the mixture fraction ξ equals the sample space variable η . Transport equations are solved for Q_α , the conditional expectation for the mass fraction of species α , and Q_T , the conditional expectation for the temperature.

The closed transport equation for the conditionally averaged species mass fractions is given by:

$$\begin{aligned} \frac{\partial Q_\alpha}{\partial t} = & -\langle u_i | \eta \rangle \frac{\partial Q_\alpha}{\partial x_i} + \langle w_\alpha | \eta \rangle + \langle N | \eta \rangle \frac{\partial^2 Q_\alpha}{\partial \eta^2} \\ & - \frac{1}{\bar{\rho} \tilde{P}(\eta)} \frac{\partial}{\partial x_i} \left(-D_t \frac{\partial Q_\alpha}{\partial x_i} \bar{\rho} \tilde{P}(\eta) \right) + S(\eta) Y_{s\alpha} - S(\eta) Q_\alpha - (1 - \eta) S(\eta) \frac{\partial Q_\alpha}{\partial \eta} \end{aligned} \quad (1)$$

The derivation of this equation set neglects fluctuations away from the conditional mean evaporation rate, written as $S(\eta) \text{ s}^{-1}$. The final three terms arise due to fuel evaporation. In order, their meaning may be understood as a source term for the species which are evaporating (or condensing). The next term may be thought of as a dilution term resulting from the addition of new matter to the gas phase. The final term represents a convective flux in mixture fraction space due to the release and dilution of mixture fraction by evaporation. Closure of the CMC spray terms requires a model for the conditional evaporation rate which is discussed below. The associated CMC temperature equation is:

$$\begin{aligned} \frac{\partial Q_T}{\partial t} = & -\langle u_i | \eta \rangle \frac{\partial Q_T}{\partial x_i} + \sum_{\alpha=1}^n \frac{h_\alpha \langle w_\alpha | \eta \rangle}{\langle c_p | \eta \rangle} + \langle N | \eta \rangle \left\{ \frac{\partial^2 Q_T}{\partial \eta^2} + \frac{1}{\langle c_p | \eta \rangle} \left(\frac{\partial \langle c_p | \eta \rangle}{\partial \eta} + \sum_{\alpha=1}^n c_{p\alpha} \frac{\partial Q_\alpha}{\partial \eta} \right) \frac{\partial Q_T}{\partial \eta} \right\} \\ & + \dot{T}_{\text{spark}}(\eta) - \frac{1}{\bar{\rho} \bar{P}(\eta)} \frac{\partial}{\partial x_i} \left(-D_t \frac{\partial Q_T}{\partial x_i} \bar{\rho} \bar{P}(\eta) \right) - (1-\eta) S(\eta) \frac{\partial Q_T}{\partial \eta} + \frac{\langle \dot{h}_{\text{evap}} | \eta \rangle}{\langle c_p | \eta \rangle} \end{aligned} \quad (2)$$

or in symbolic form,

$$\frac{\partial Q_T}{\partial t} = T_{cv} + T_c + T_m + T_{\text{spark}} + T_{tf} + T_{\text{spray1}} + T_{\text{spray2}}. \quad (3)$$

Thus the rate of change of Q_T is attributed to convection T_{cv} , with the conditional velocity $\langle u_i | \eta \rangle$ given by the linear model [3]. The remaining terms on the right hand side of the conditional averaged temperature equation refer to chemical reaction T_c , molecular mixing T_m , energy deposition due to spark ignition T_{spark} , and the turbulent flux transport T_{tf} . T_{spray1} has a similar role to the convective term Eq. 1, while T_{spray2} is a conditional enthalpy source term analogous to the fifth term on the right hand side of Eq. 1.

In common with previous work [6], the conditional scalar dissipation rate $\langle N | \eta \rangle$ is modelled using the Amplitude Mapping Closure (AMC) model [11]. The conditional expectation of the chemical source term T_c was closed at first order using the expectations for the conditional temperature and mass fractions.

The first order CMC has been two way coupled with a thoroughly verified commercial RANS CFD solver, employing its standard Lagrangian spray transport and evaporation models [12]. The range of turbulent time scales expected in the spray ignition experiment is small compared with the overall time of the flow evolution. The use of unsteady RANS therefore provides a prediction of the ensemble averaged flow evolution in response to ignition. Details of the fractional step and gridding procedures used are given in ref. [10]. In all cases tests showed that propagation of the conditional flame fronts was adequately resolved in time and space. The CFD variables needed by the CMC solution were averaged over the relevant volume, weighted by the mixture fraction probability density function. A β -function PDF shape, scaled between zero and the saturation mixture fraction (found as an area weighted average for the droplets in each CMC cell), was presumed based on the modelled mean and variance of mixture fraction. The AMC conditional scalar dissipation profile was then also scaled between zero and the saturation mixture fraction.

Spray term modelling

In a spray fuelled flow the equation for the mean mixture fraction [12] contains the mean unconditional evaporation rate, $\rho S \text{ kg.m}^{-3} \text{s}^{-1}$. In the simulations conducted in this work this quantity is directly available from the Lagrangian spray model.

The CMC equations require modelling for the conditional evaporation rate $S(\eta)$ and for the conditional heat transfer to the liquid phase, $T_{\text{spray}2}$. Four approaches for the treatment of these terms are now discussed. The first treatment of the conditional evaporation rate considered is to assume all inter-phase mass transfer occurs at a value of the fuel's saturation mixture fraction based on the modelled droplet surface temperatures. The conditional evaporation rate profile is then found as either a combination of delta function sources at the saturation mixture fraction values for the droplets found in that CMC cell, or a single delta function source at a mixture fraction representative of the saturation values found in that cell.

The second approach represents a special case of approach one, where it is assumed that all evaporation occurs due to boiling and therefore that all mass transfer occurs at $\xi=1$. Examination of Eqs. 1 and 2 shows that in this case all the spray terms cancel except the conditional heat transfer to the liquid phase, $T_{\text{spray}2}$. This assumption may be valid for evaporation in regions where the gas temperature is well above the fuel's boiling point.

The third and fourth approaches are based on the work of Réveillon and Vervisch [13] and Sreedhara and Huh [14] respectively. Both are motivated by direct numerical simulation (DNS) results for evaporation of sub-Kolmogorov scale droplets in turbulent flows. These are used to propose analytical expressions for the conditional evaporation rate profiles. The earlier work by Réveillon and Vervisch resulted in the "Single Droplet Model" (SDM) and the later work produced a simpler linear profile for the conditional evaporation rate. The ensemble average evaporation rates reported in these works appear to have been compiled according to the gaseous mixture fraction recorded for the DNS volume where each droplet resides. This presents a discrepancy with the reasoning of the first two approaches for which it was argued that the droplet surface mixture fraction is the quantity on which the evaporation rate should be conditioned. Approaches one and two have been employed during this study.

The evaporation terms arising in the variance equation may be written:

$$\bar{\rho} \dot{\bar{\xi}}_{\text{evap}}^{\prime\prime 2} = 2\langle \rho \xi'' S \rangle (1 - \bar{\xi}) - \langle \rho \xi''^2 S \rangle \quad (4)$$

The presumed mixture fraction PDF and a model for the conditional evaporation rate then yield the remaining unclosed terms $\langle \rho \xi'' S \rangle$ and $\langle \rho \xi''^2 S \rangle$ [13].

Spark Ignition Modelling

Spark ignition has been approximated by a transient energy deposition at the spark location, attempting to represent the basic spark properties: dimension, duration and energy without providing a description of the many complicated physical processes inherent to practical ignition. The power of energy deposition has been modelled as uniform in time and space within a spherical volume with diameter equal to the electrode spacing.

The CMC requires additional modelling for the distribution of the energy deposition across mixture fraction space. Two approaches are proposed:

In the first approach the specific enthalpy deposition rate is assumed to be uniform across mixture fraction space. This model has the property that the different compositions experience differing temperature histories according to their heat capacities and chemical evolution.

$$\dot{T}_{\text{spark}}(\eta) = \frac{1}{\langle c_p | \eta \rangle} \frac{\partial h}{\partial t} \quad (5)$$

The second approach is based on an argument that the temperature attained by a fuel-air mixture inside the spark gap is largely prescribed by a balance between the electrical energy input and the heat lost to the electrodes and through radiation. As such the temperature would

not be as strong a function of mixture fraction. In the absence of chemical change at the $\eta=0$ and $\eta=1$ boundaries of mixture fraction, the following expression for the conditional temperature source gives equal temperature increments at $\eta=0$ and $\eta=1$, and maintains a linear variation of enthalpy between the two boundaries.

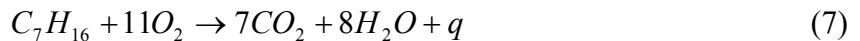
$$\dot{T}_{spark}(\eta) = \frac{1}{\langle c_p | \eta \rangle} \frac{\partial h}{\partial t} \left[\frac{(1-\eta)\langle c_p | \eta = 0 \rangle + \eta \langle c_p | \eta = 1 \rangle}{\int_{\xi}^1 ((1-\eta)\langle c_p | \eta = 0 \rangle + \eta \langle c_p | \eta = 1 \rangle) P(\eta) d\eta} \right] \quad (6)$$

In the absence of detailed experimental or numerical simulation results the practical and technical properties of both models are discussed below in the context of an idealised one dimensional turbulent spark ignition example.

Partially Premixed Reaction Model For *n*-Heptane

In the current modelling study of spray flame ignition and propagation the principal quantity needed from the chemical reaction model is the heat release rate. To this end the simple one step reaction model proposed by Fernández-Tarrazo et al. [15] has been used. The model expresses the heat of reaction and the Arrhenius activation temperature as functions of equivalence ratio. This achieves the correct laminar premixed flame speed for methane-air flames and realistic diffusion flame structures even close to extinction [15]. In this work a set of model constants have been developed for *n*-heptane combustion [10].

The *n*-heptane oxidation model is given by,



with a global reaction rate (mol.cm⁻³s⁻¹) of the form,

$$\omega = Be^{-T_a/T} \Gamma_{C_7H_{16}} \Gamma_{O_2} \quad (8)$$

and the heat release due to complete oxidation of one mole of fuel given by,

$$q_0 = h_{C_7H_{16}} - 7h_{CO_2} - 8h_{H_2O} = 5401 kJ.mol^{-1}. \quad (9)$$

The reduced heat release resulting from incomplete combustion at rich equivalence ratios is modelled by,

$$\begin{cases} \phi \leq 1 : q/q_0 = 1 \\ \phi > 1 : q/q_0 = 1 - \alpha(\phi - 1). \end{cases} \quad (10)$$

The parameters selected in order to model partially premixed *n*-heptane combustion at atmospheric conditions were $\alpha=0.18$, $T_{a0}=15000K$ and $B=2.4 \times 10^{14} \text{cm}^3.\text{mol}^{-1}\text{s}^{-1}$ as discussed in ref. [10]. T_a was expressed as,

$$\left\{ \begin{array}{l} \phi \leq 0.74 : T_a / T_{a0} = 1 + 1.6948(\phi - 0.74)^2 \\ 1.13 \geq \phi > 0.74 : T_a / T_{a0} = 1 \\ \phi > 1.13 : T_a / T_{a0} = 1 + 0.0092(\phi - 1) + 0.9423(\phi - 1.13)^2. \end{array} \right. \quad (11)$$

This fit produces the variation of premixed laminar flame speed with equivalence ratio shown in Fig. 3

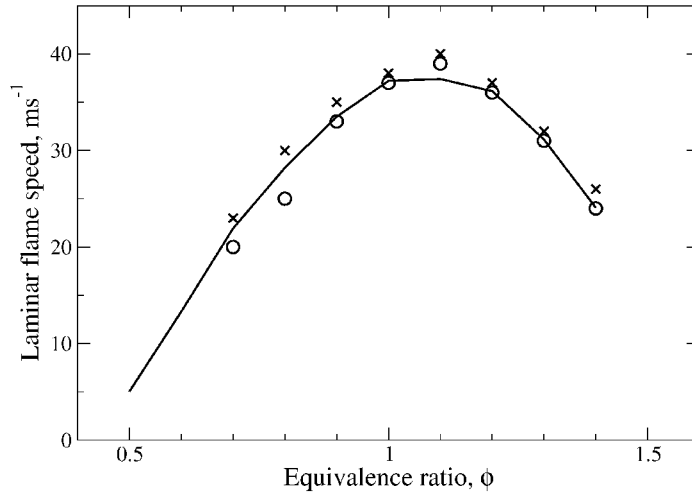


Figure 3. The modelled flame n-heptane laminar flame speed versus equivalence ratio at 1bar and 300K, compared to experimental measurements by Huang et al. (crosses) [16], and Davis and Law (circles) [17].

The Swirl Stabilised Spray Burner

The air flow rate used for the experiment simulated in this work was $479.9 \text{ l}.\text{min}^{-1}$, passing through a vane swirler as indicated in Fig. 1 with a 60° metal angle at exit. The simulation inlet boundary condition coincides with the swirler exit plane. A flow angle of 60° is imposed.

The specification for the pressure swirl fuel injector with 5 bar injection pressure and a $150\mu\text{m}$ orifice indicates that a spray Sauter mean diameter of $30\mu\text{m}$ can be expected. The droplet diameter distribution is presumed using the Rosin-Rammler function (with $q = 2$) [18]. The initial droplet trajectories are randomly distributed within a hollow cone from 55° - 65° internal angle. The measured flow rate of n -heptane, $0.0366 \text{ l}.\text{min}^{-1}$, indicates an extremely high injector discharge coefficient of 0.9 as defined by Lefebvre [19], therefore the spray injection speed has been estimated as 34ms^{-1} .

Results and Discussion

One Dimensional Test Problem

A one dimensional configuration was developed with similar spray, turbulence and spark parameters to the spark location in the ignition experiment. A 1mm thick planar spark, with a duration of $400\mu\text{s}$ (note that the quenching distance for a planar flame is approximately half that of its spherical equivalent [20]) and an energy of deposition of 2kJ.m^{-2} . Due to the absence of convection this is less than the 5MJm^{-3} energy density used in the ignition experiment simulation. A constant turbulent viscosity of $\mu_T=0.005\text{m}^2\text{s}^{-1}$ is imposed. A stoichiometric quantity of liquid n -heptane is introduced in the form a uniform $30\mu\text{m}$ droplet mist.

Both spark models Eq. 5 and Eq. 6 are tested, with the full two phase CMC model. Figure 4 shows that while the sparks result in differing conditional temperature profiles at completion of the energy deposition, differences within the propagating flame front are very

small after five times the spark duration. This is especially true around stoichiometry where the turbulent flame propagation rate is largely controlled.

The effect of the evaporative terms in the two phase CMC model have been explored by comparing two simulations, one with the evaporative source term in the mixture fraction variance equation and one without. Both simulations model the spark using Eq. 6. The comparison is shown in Fig. 5. The outcome of the solution is highly dependent on the modelling for the variance source term and the resulting mixture fraction PDF shape. The case which includes the variance source term predicts a wider PDF, with little mass close to stoichiometry. This results in lower unconditional flame temperatures and lower flow acceleration across the flame. Figure 5b clearly shows the difference in the role of the conditional convection term. In addition, the conditional scalar dissipation rate modelling is dependent on the modelled mixture fraction variance and while its value was always below the quenching threshold the inclusion of the variance term resulted in values up to an order of magnitude higher (not shown).

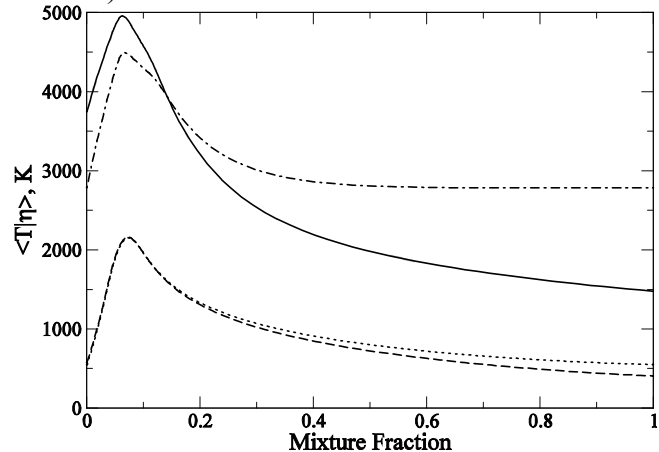


Figure 4. Conditional temperature profiles at the spark centre at completion of the energy deposition (Eq. 5: solid); Eq. 6: (dot-dashed), and at the location of peak stoichiometric heat release once five spark durations have elapsed, (Eq. 5: dashed; Eq. 6: dotted).

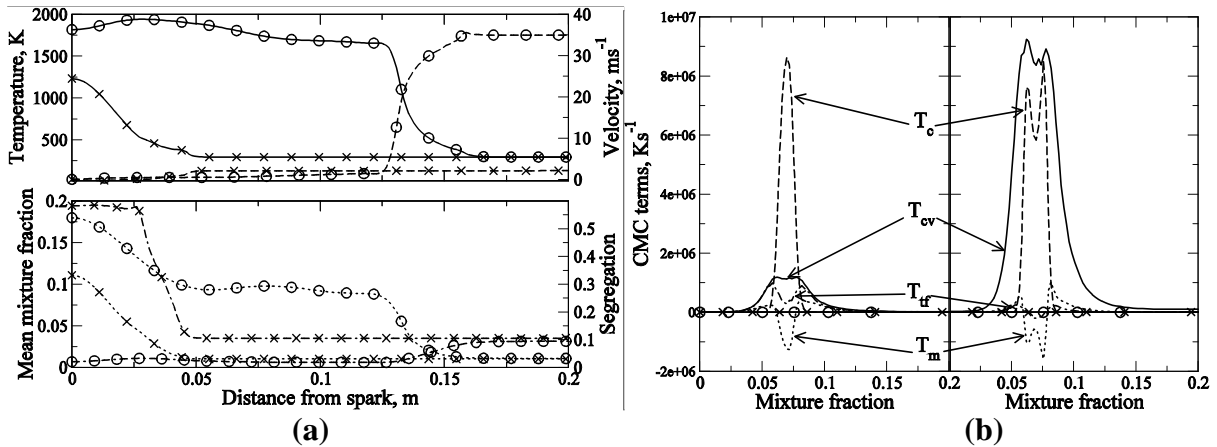


Figure 5(a) Spatial profiles through the spray flame after $80\mu s$, with the variance source term (crosses) and without it (circles). Solid lines: Favre temperature; dashed: mean flow velocity; dotted: mean mixture fraction; dot-dashed: segregation coefficient, $\langle \xi''^2 \rangle / [\langle \xi \rangle (1 - \langle \xi \rangle)]$.

Figure 5(b) Profiles of the conditional temperature equation source terms for the points of peak stoichiometric heat release for the variance source term case (left) and the no-variance source term case (right). Terms are labeled according to Eq. 3, additionally $T_{\text{spray}1}$ is marked with circles, $T_{\text{spray}2}$ with crosses.

According to the conditional evaporation rate model employed, the CMC evaporation terms are only active at the mixture fraction saturation value. The saturation mixture fraction was above 0.98 by the location of the peak heat release so that the net effect of the

evaporative CMC terms was negligible. The heat transfer term is significant. However since it acts at a mixture fraction far away from stoichiometry, use of the AMC dissipation rate profile means that it has little effect on the flame propagation.

SprayBurner: Unreacting flow

The simulation is conducted using the Gibson-Launder Reynolds Stress closure implemented in STAR-CD [12] without modification ensuring sufficient resolution to give grid independent solutions. The simulated mean and root mean square axial and azimuthal velocity components are compared with Laser Doppler Anemometry, LDA, measurements at two down stream distances in Fig. 6. Reasonable agreement is achieved for the mean velocity quantities however the comparison suggests that the velocity fluctuations are significantly over predicted. Despite the limited accuracy of Reynolds Averaged Navier Stokes approach it has been used throughout this work and due care must be exercised when interpreting the results.

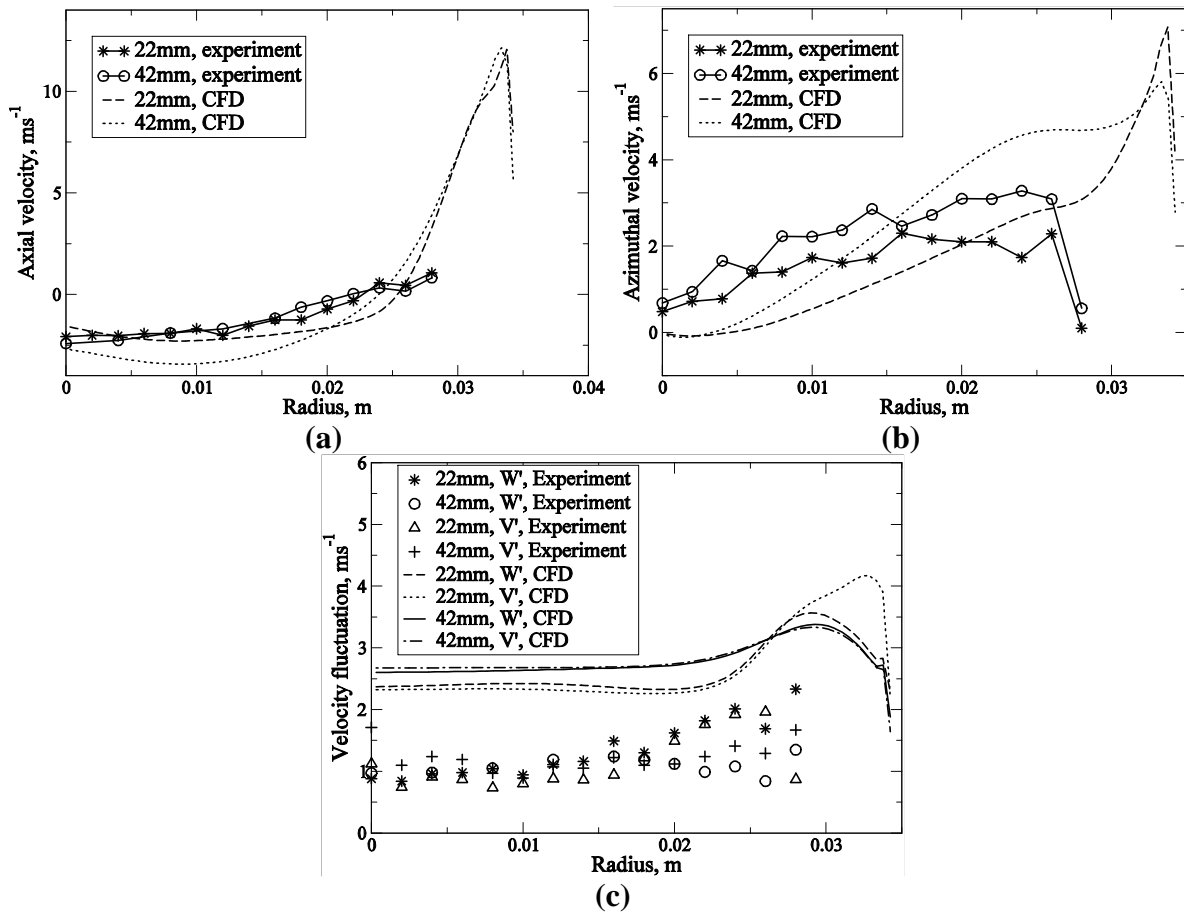


Figure 6. A comparison of experimental LDA velocity measurements [1] with inert simulations across the radius at 22mm and 42mm downstream from the bluff body. **(a):** Mean axial velocity; **(b):** Mean azimuthal velocity; **(c):** RMS axial (W) and azimuthal (V) velocities.

Figure 7 indicates a qualitative agreement between the observed and predicted spray patterns in the inert flow. The initial velocity and diameter distributions have been estimated based on the injector specification however it would be desirable to be able to specify the distribution directly based on experimental measurements.

Due to the high vapour pressure of *n*-heptane at room temperature significant fuel evaporation occurs prior to ignition with largely uniform region of fuel vapour approximately 15mm in length with $\xi=0.045$ adjacent to the downstream face of the bluff body.

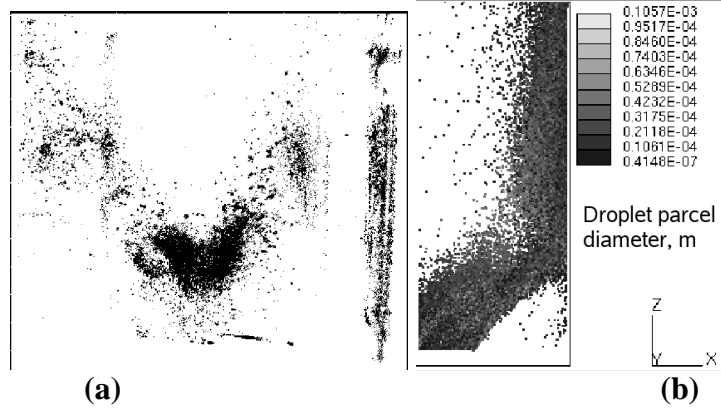


Figure 7(a): Instantaneous cross sectional Mie scattering image of the non-burning fuel spray [1]. Image dimensions 70mm wide and 80mm high; (b): A predicted droplet parcel distribution prior to ignition, image dimensions: 35mm wide and 80mm high.

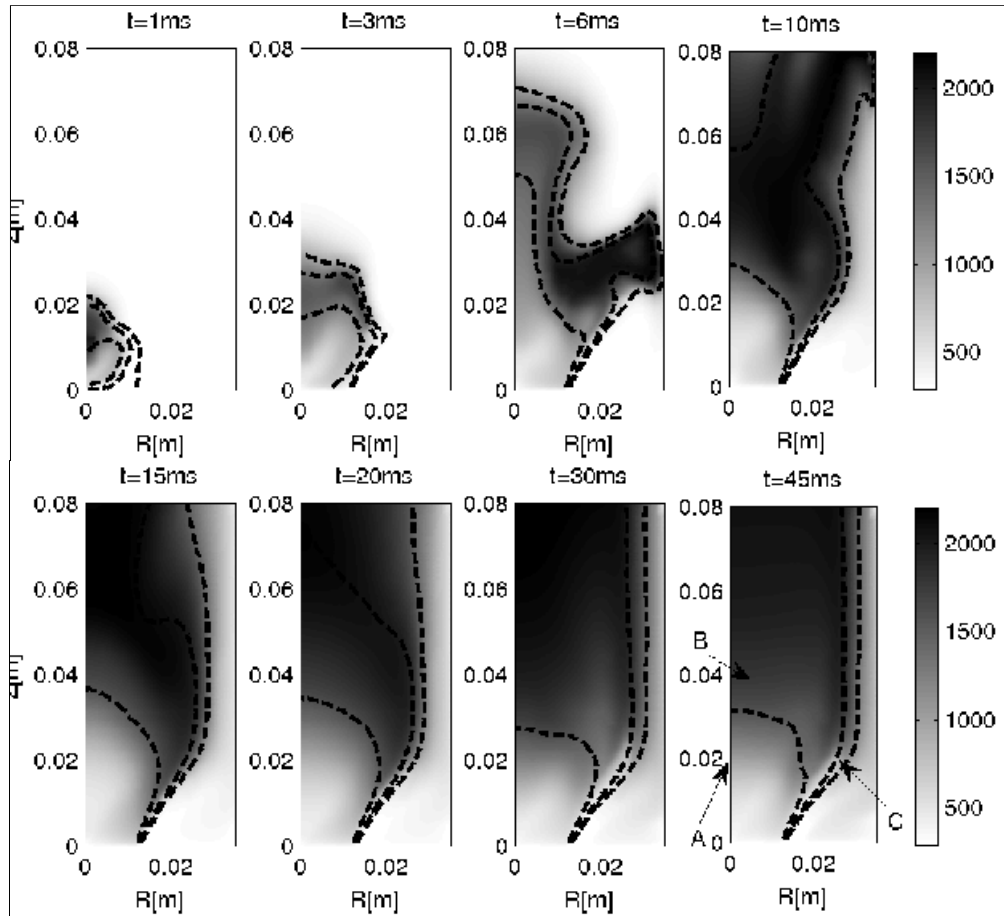


Figure 8. The simulated unconditional temperature evolution in Kelvin. The dashed black lines are iso-lines of mean mixture fraction, the innermost representing the rich flammability limit ($\xi=0.199$), the next line is stoichiometric ($\xi=0.062$) and the outer line represents the lean limit, ($\xi=0.035$).

Spray Burner: Ignition Simulation

The CMC model has been used to simulate the ignition event shown in Fig. 2, which gives an indication of the instantaneous flame positions viewed across the flow. The CMC results presented in this section neglect the contributions of the evaporative source terms in the conditional species and energy equations and the mixture fraction variance equation. This is considered a reasonable approximation because the high temperatures within the flow lead to an *n*-heptane saturation condition which is generally close to pure fuel. Therefore the

evaporation has a limited effect on the evolution of the flame's conditionally averaged quantities close to stoichiometry. Contours of the simulated mean temperature and mean heat release rates are shown in Figs. 8 and 9. It must be highlighted that the experimental images record instants during the flame evolution while the RANS-CMC predictions represent an average of an ensemble of similar experiments. A qualitative comparison with the experimental images suggests that, in common with coupled RANS-CMC simulations of other ignition-propagation problems [4,10], the current model over-predicts the rate of flame spread. However the predicted flame propagation speed and stabilised flame shape broadly agrees with that inferred from the fast camera images, aside from differences in the timings.

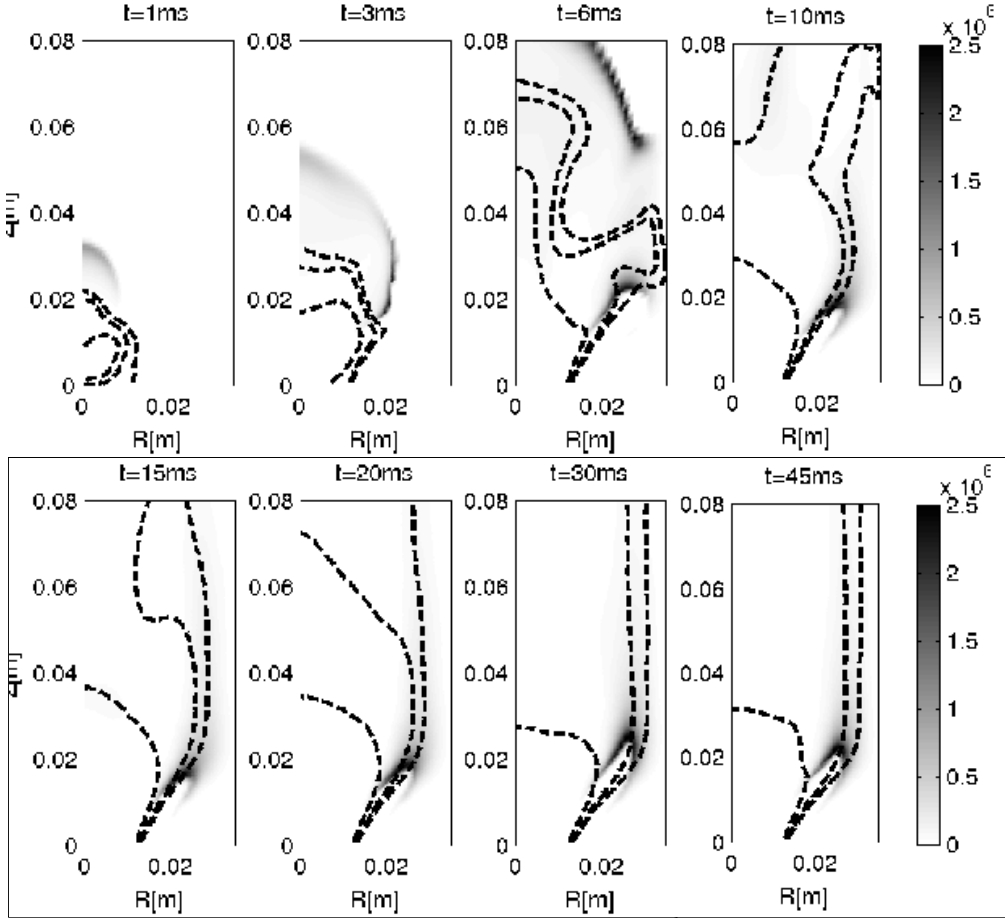


Figure 9. The simulated unconditional heat release rate evolution, (Ks^{-1}). Iso-lines of mean mixture fraction are shown as in Fig. 8.

The simulated heat release rate indicates that the flame propagates ahead of the mean contour corresponding to the lean flammability limit (which itself moves due to thermal expansion and evaporation). This is possible due to the low gradient of mean mixture fraction and a high mixture fraction variance providing significant flammable mixture at the flame front. However a large diffuse reaction zone persists inside the inflamed region.

As the flame front approaches the enclosure a downstream portion splits off and propagates out of the enclosure. The upstream portion propagates against the in-flow and eventually stabilises, marking the furthest penetration of unreacted flow from the annulus.

The ignition and stabilisation process is accompanied by a large disruption to the flow and mixing field which may be inferred from the mean mixture fraction contours in Fig. 8. In particular, evaporation close to the injector creates a region so rich, with temperatures sufficiently low that the spray penetrates far into the burner.

Figures 10a and 10b show the spatial profiles of the CMC temperature equation on axial and radial transects respectively through point C, ($r = 0.026m$, $z = 0.0236m$) as indicated in

Fig. 8. The stoichiometric conditional temperature profiles show the presence of the inflow, which is surrounded by regions of high heat release and mixing of the conditional quantities. Figure 10c shows the conditional temperature and the CMC temperature equation terms at point C. The conditional heat release shows two peaks, one close to stoichiometry and one close to the rich flammability limit. Such a heat release profile is consistent with the occurrence of a double flame structure. The heat release is largely offset by molecular dissipation and the convection term.

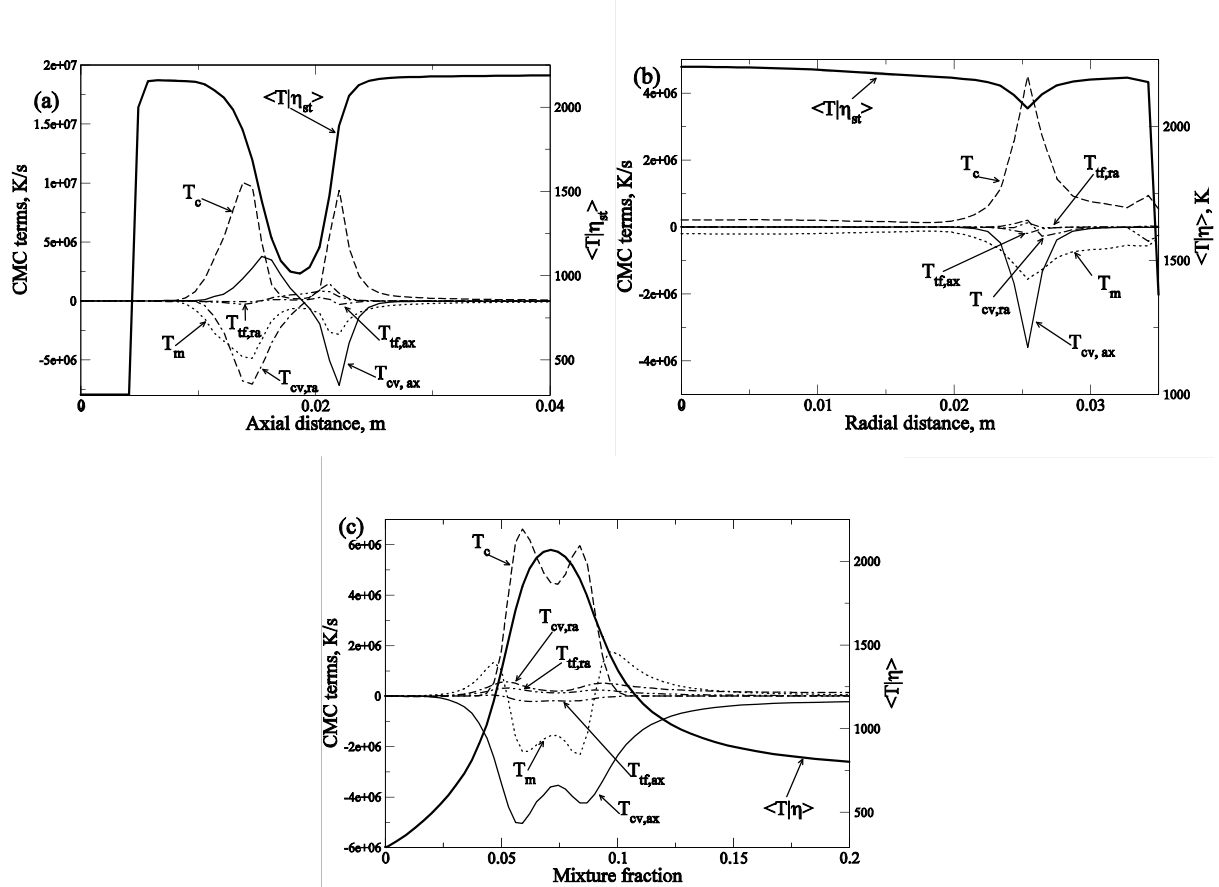


Figure 10. The conditional temperature and the balance of terms in the CMC temperature equation 45ms after ignition. (a): Spatial profiles along an axial transect through point C; (b) Spatial profiles along a radial transect through point C; (c) Mixture fraction space profiles at point C.

Conclusions

The first order, elliptic CMC model has been implemented and used to simulate the complete ignition process up to flow stabilisation in a turbulent bluff body stabilised spray burner. This represents a new and industrially relevant application for the CMC model. The simulated rate of turbulent flame propagation greatly exceeds that observed experimentally. This has been attributed to limitations of the first order reaction rate closure, and a possible inability of the coupled RANS-CMC approach to adequately describe the transient large scale turbulent motions and their interaction with the heat release. In addition the propagation rate is highly sensitive to mixture fraction PDF, hence modelling of the variance equation and scalar dissipation are critical.

A complete CMC model for spray fuelled combustion is presented whose terms are illustrated through a simple spray ignition example. It is seen that net effect of the two phase terms in the CMC equation are not generally significant, apart from the term representing the heat transfer to the liquid phase. However the importance of modelling for the evaporative

source term in the mixture fraction variance equation has been demonstrated. The modelling of the conditional scalar dissipation rate in the presence of evaporation also needs attention.

Two CMC models for forced ignition are presented and compared. These models produce short lived differences in the evolution of the conditional profiles, however after around 5 spark times they ultimately result in very similar flame progression in the test case considered. It is noted that Eq. 5 is simpler to implement. An *n*-heptane version of the Fernández-Tarrazo et al. [Fernandez06] one step reaction rate model has been developed and presented.

There is some evidence to suggest that first order, singly conditioned CMC may be inadequate for propagating flow problems as considered here [21], and that a doubly conditioned approach could be more suitable. It is expected that many aspects of the current predictions could be improved through use of Large Eddy Simulation (LES) coupled with an advanced turbulent reacting flow model. In contrast with the RANS approach, LES predicts the evolution of individual ignition events without ensemble averaging. Therefore repeated application of LES under similar ignition conditions has the potential to provide information about the statistics of combustor ignitability.

References

- [1] Marchione, T., Ahmed, S.F., Balachandran, R., Mastorakos, E, *21st ICDERS*, Poitiers, France, July 2007, submitted.
- [2] Marchione, T., Ahmed, S.F., Mastorakos, E, *Fifth Mediterranean Combustion Symposium*, Monastir, Tunisia, September 2007, submitted.
- [3] Klimenko, A.Y., and Bilger, R.W, *Prog. Energy Combust. Sci.* 25, 595-687, (1999).
- [4] Richardson, E.S., and Mastorakos, E, *Third European Combustion Meeting*, Chania, Crete, April 2007 pp.8/15.
- [5] Devaud, C.B., and Bray, K.N.C, *Combust. Flame*, 132, 102-114, (2003).
- [6] Wright, Y.M., de Paola, G., Boulouchos, K., Mastorakos, E., *Combust. Flame*, 143, 402-419, (2005).
- [7] Kim, W.T., and Huh, K.Y, *Proc. Comb. Inst.*, 29, 569-575, (2002)
- [8] Rogerson, E, PhD thesis, University of Sydney, (2006).
- [9] Smith, N.S.A., Cha, C.M., Pitsch, H., Oefelein, J.C, *CTR Proc. Summer Prog.*, NASA Ames, pp.207-218, (2000).
- [10] Richardson, E, PhD thesis, University of Cambridge, (2007).
- [11] O'Brien, E.E., and Jiang, T.L, *Phys. Fluids*, 3, 3121-3123, (1991).
- [12] STAR-CD *Methodology Guide*, version 3.26, 2005. CD adapco.
- [13] Réveillon, J., Vervisch, L, *Combust. Flame*, 121, 75-90, (2000).
- [14] Sreedhara, S., Huh, K.Y, *Proc. Comb. Inst.*, 31, 2335-2342, (2006)
- [15] Fernández-Tarrazo, E., Sánchez, A., Liñán, A., Williams, F.A, *Combust. Flame*, 147, 32-38, (2006).
- [16] Huang, Y., Sung, C.J., Eng, J.A, *Combust. Flame*, 139, 239-251, (2004).
- [17] Davis, S.G., and Law, C.K, *Combust. Sci. Tech*, 140, 427-449, (1998).
- [18] Rosin, P., and Rammler, E, *The Journal Inst. Fuel*, 7, 29-36, (1933).
- [19] Lefebvre, A.W., *Gas Turbine Combustion*, Mc Graw-Hill, 1999, p. 238
- [20] Richardson, E.S., Mastorakos, E, *Combust. Sci. Tech*, 179, 293-317, (2006).
- [21] Richardson, E.S., Chakraborty, N., Mastorakos, E, *Proc. Combust. Inst.*, 31, 1683-1690, (2007).